Heterologous Expression and Purification of the Serotonin Type 4 Receptor from Transgenic Mouse Retina[†]

David Salom,[‡,§] Nan Wu,[‡,§] Wenyu Sun,[‡,§] Zhiqian Dong,[‡] Krzysztof Palczewski,*[,||] Steven Jordan,[⊥] and John A. Salon*[,⊥]

Polgenix Inc., 11000 Cedar Avenue, Suite 260, Cleveland, Ohio 44106, Department of Pharmacology, Case Western Reserve University, Cleveland, Ohio 44106, and Amgen Inc., Thousand Oaks, California 91320

Received September 30, 2008; Revised Manuscript Received November 3, 2008

ABSTRACT: Recent breakthroughs in the solution of X-ray structures for G protein-coupled receptors (GPCRs) with diffusible ligands have employed extensively mutated or recombined receptor fusion proteins heterologously expressed in conventional in vitro cell-based systems. While these advances now show that crystallization of non-rhodopsin members of this superfamily can be accomplished, the use of radically modified proteins may limit the relevance of the derived structures for precision-guided drug design. To better enable the study of native GPCR structures, we report here efforts to engineer an in vivo expression system that harnesses the photoreceptor system of the retina to express heterologous GPCRs with native human sequences in a biochemically homogeneous and pharmacologically functional conformation. As an example, we show that the human 5HT4 receptor, when placed under the influence of the mouse opsin promoter and an opsin rod outer segment (ROS) targeting sequence, localized to ROS of transgenic mouse retina. The resulting receptor protein was uniformly glycosylated and pharmacologically intact as demonstrated by immunoblotting and radioligand binding assays. Upon solubilization, the retinal 5HT4 receptor retained the binding properties of its initial state in retinal membranes. With the engineered T7 monoclonal epitope sequence, the solubilized receptor was easily purified by one-step immunoaffinity chromatography and the purified receptor in detergent solution preserved its ligand binding properties. This expression method may prove generally useful for generating functional, high-quality GPCR protein.

The importance of G protein-coupled receptors (GPCRs)[1] in the field of drug discovery is well-documented. Despite this proven tractability, however, only a small percentage of the overall GPCR superfamily is explicitly targeted by currently marketed drugs (*1, 2*). This apparent paradox may, in part, stem from the fact that the molecular diversity of corporate screening libraries, which serve as the starting point for drug discovery, is typically limited to tightly clustered domains of chemical space that represent medicinal chemistry efforts aimed at previously explored targets. Thus, most of today's drug discovery is biased toward historical campaigns and revolves around well-trodden (i.e., non-novel) pharmacologies. It follows that ligands targeting structurally diverse members of the GPCR superfamily or which are meant to function via nonconventional modes of action largely remain to be identified. This situation could theoretically be addressed by a de novo approach to drug design that employs the complementary pharmacophore structure of the targeted receptor itself. Unfortunately, such a rational approach is hampered by the lack of three-dimensional (3D) coordinates for GPCR targets and the underlying difficulty of generating high-quality protein crystals for their elucidation.

Recent developments, however, suggest that these difficulties may be overcome. Specifically, the recent publication of medium-resolution X-ray structures for a human β_2-adrenergic receptor T4 lysozyme and A_{2A}-adenosine fusion protein, a mutated turkey β_1-adrenergic receptor, and a mutated form of rhodopsin demonstrates the feasibility of producing diffracting crystals for GPCR protein(s) that are expressed in and purified from heterologous hosts (*3* and references therein). While these reports constitute encouraging breakthroughs and may provide important insights into

[†] This research was supported in part by U.S. Small Business Innovation Research (SBIR) Grant R44MH068919 from the National Institute of Mental Health and Grant R44DA016476 from the National Institute of Drug Abuse, National Institutes of Health.

* To whom correspondence should be addressed. J.A.S.: Department of Molecular Pharmacology, MS 29-M-A, Amgen Inc., One Amgen Center Drive, Thousand Oaks, CA 91320-1799; phone, (805) 447-6442; e-mail, jsalon@amgen.com. K.P.: Department of Pharmacology, School of Medicine, Case Western Reserve University, 10900 Euclid Ave., Cleveland, OH 44106-4965; phone, (216) 368-4631; fax, (216) 368-1300; e-mail, kxp65@case.edu.

[‡] Polgenix Inc.

[§] These authors contributed equally to this work.

[||] Case Western Reserve University.

[⊥] Amgen Inc.

[1] Abbreviations: 5HT4R, 5-hydroxytryptamine receptor type 4; mAb, monoclonal antibody; AP, alkaline phosphatase; GPCR, G protein-coupled receptor; ROS, rod outer segment(s); Zacopride, 4-amino-*N*-1-azabicyclo[2.2.2]oct-3-yl-5-chloro-2-methoxybenzamide; GR113808, 1-methyl-1*H*-indole-3-carboxylic acid (1-{2-[(methylsulfonyl)amino]ethyl}-4-piperidinyl)methyl ester; GR125487, 5-fluoro-2-methoxy-(1-{2-[(methylsulfonyl)amino]ethyl}-4-piperidinyl)-1*H*-indole-3-methylcarboxylate; RS23597-190, 3-(piperidin-1-yl)propyl 4-amino-5-chloro-2-methoxybenzoate; SB 203186, 1-piperidinylethyl-1*H*-indole-3-carboxylate; Tropisetron, (3-endo)-8-methyl-8-azabicyclo[3.2.1]oct-3-yl 1*H*-indole-3-carboxylic acid ester; β_2-AR, β_2-adrenergic receptor; DAPI, 4′,6-diamidino-2-phenylindole; WT, wild type; BSA, bovine serum albumin; PCR, polymerase chain reaction; RT-PCR, reverse transcriptase polymerase chain reaction.

10.1021/bi8018527 CCC: $40.75
Published on Web 11/20/2008

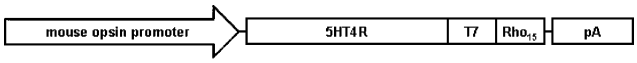

FIGURE 1: 5HT4R-T7-Rho_{15} cDNA construct. Expression of this construct is driven by a 5 kb mouse opsin promoter (left) followed by in-frame human 5HT4R cDNA with T7 and Rho_{15} tags. The 3′-untranslated region contains a SV40 polyadenylation signal.

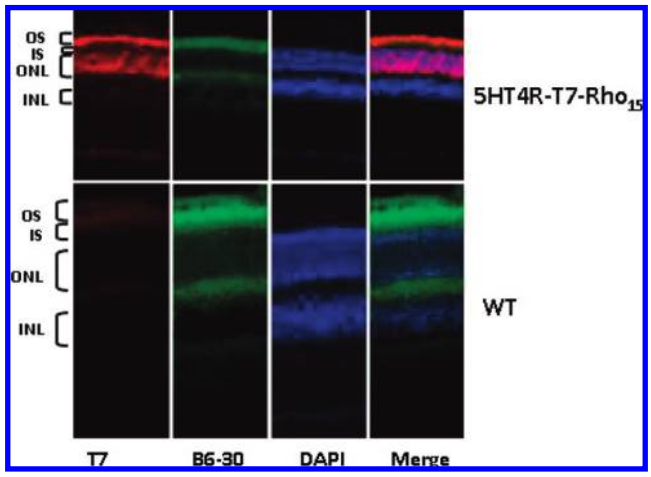

FIGURE 2: Immunostained retinal sections from 5HT4R-T7-Rho_{15} transgenic mice. Top and bottom panels show retinal sections from 5HT4R-T7-Rho_{15}-expressing mice and WT littermates, respectively. Immunostaining reveals the expression of opsin (B6-30 mAb, green) and 5HT4R-T7-Rho_{15} (T7 mAb, red) in the retinas of 5HT4R-T7-Rho_{15} transgenic mice but only opsin in WT controls. Nuclei were stained with DAPI (blue). Abbreviations: OS, outer segments; IS, inner segments; ONL, outer nuclear layer; INL, inner nuclear layer.

the gross structural features of GPCR function, the use of radically modified GPCR proteins for crystal generation may undermine the usefulness of the resulting coordinates for elucidation of details of pharmacophore binding at a precision needed for rational drug design (*3*).

A somewhat different tack employing unmodified GPCR sequences is suggested by work done in determining the 3D structure of native rhodopsin isolated from bovine retina (*4*−*7*). This advance took advantage of the naturally enriched levels of rhodopsin that occur in the retina and the fact that this protein is uniformly glycosylated to provide large amounts of homogeneous protein for crystallization (*8*). By extension, we have proposed that the unique biosynthetic pathways of the retina's rod cells may be exploited as a "bioreactor" to produce nascent heterologous GPCR proteins for purification and crystallization. Proof of this concept has been reported with *Drosophila* and *Xenopus* systems (*9*−*11*), and we have extended it to the mouse to ensure that any subtleties specific to mammalian protein expression and processing are incorporated into the resulting protein (*12*).

We have previously reported success with this approach using the adenosine A1 receptor (AA1R) as the heterologous target but also noted the occurrence of aberrations in retinal integrity with an accompanying diminution in the overall level of protein expression (*12*). Despite these difficulties, the exogenous AA1R clearly localized to the retinal photoreceptors, where it appeared to be homogeneously glycosylated and pharmacologically intact. This suggested that the overall goal of employing rod cells as an in vivo expression system was achievable. To explore this system more fully, we focus here on the serotonin type 4 receptor (5HT4R) and document the ability to express and purify this receptor from genetically engineered mouse tissue. The pharmacological characteristics of the receptor, in both membrane- and detergent-solubilized form, compare favorably with those of analogous preparations from conventional cell culture expression systems, supporting the relevance of the rod cell-expressed conformations for structural studies.

MATERIALS AND METHODS

Constructs for Generating Transgenic Mice and Transfected Cells. The transgenic mouse expression plasmid for 5HT4R-T7-Rho_{15} was constructed as follows. A pXOP-C1(−) vector originally constructed to target retinal expression in *Xenopus laevis* (*9*) was cut with *Not*I/*Xho*I to remove the *Xenopus* opsin promoter sequence which was then replaced with the 5 kb mouse rhodopsin promoter (*13*−*15*). DNA sequences encoding an 11-amino acid tag (MASMTGGQQMG) corresponding to the N-terminal region of the major capsid protein of T7 bacteriophage (T7) and a 15-amino acid Rho_{15} tag (SATASKTETSQVAPA) containing the ROS targeting sequence of mouse opsin were then inserted to produce the parental mouse expression vector pNova-T1 (*16, 17*). The full-length coding sequence for human 5HT4bR was generated by reverse transcriptase polymerase chain reaction (RT-PCR) using *pfu* polymerase (Stratagene, La Jolla, CA). Amplimers designed from the GenBank accession file of human 5HT4bR included a perfect Kozak site prior to the start codon. The blunt-ended amplified product was inserted into the *Pme*I site of pNova-T1 to generate the recombinant vector, pNova-T1-5HT4R-T7-Rho_{15}, which was then used to generate the transgenic mouse lines.

For TREx-293 (Invitrogen Corp., Carlsbad, CA) transfection, the 5HT4R-T7-Rho_{15} construct was inserted into a pcDNA4/TO vector (Invitrogen) for expression under the CMV promoter.

Genotyping. Genotyping of transgenic mice was done by polymerase chain reaction (PCR). The primers used were (in the forward direction) 5HT4R-F (5′-CCACCATGGACAAACTTGATGCTAATGTG) corresponding to the start of the coding region and (in the reverse direction) MOPS-A1 (5′-TTAGGCTGGAGCCACCTGGC) corresponding to the end of the Rho_{15} tag. Amplification was performed on an ABI 9700 instrument under denaturing conditions at 94 °C for 2 min, then 40 cycles at 94 °C for 20 s, 55 °C for 20 s, and 72 °C for 1 min followed by extension at 72 °C for 7 min, and a final soak at 4 °C.

Breeding of Transgenic Mice for Tissue Harvest. Genotyped positive F1 founders were used to establish breeding stock for subsequent animal production. Transgenic breeders were crossed with WT mice to produce a mixed population of offspring that was shown to be 50% positive for the transgene by spot genotype testing. Production scale breeding did not exclude the sibling WT offspring from the tissue harvesting campaigns.

In Vivo Antagonist Treatments. Lactating mice with 1-week-old pups were provided with drinking water containing 10 μM 5HT4R antagonist RS39604 for 2 weeks. Pups were sacrificed at 3 weeks of age, and their eyes and retinas were collected and processed for immunocytochemistry and immunoblotting, respectively.

Histology and Immunocytochemistry. Procedures for these studies have been previously reported (*18*−*20*). Briefly,

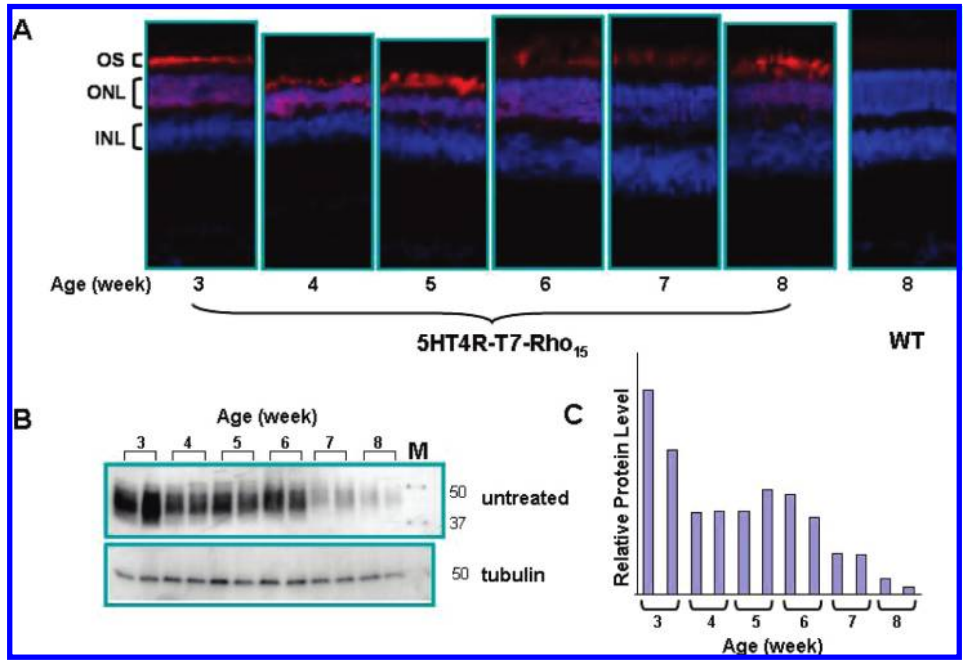

FIGURE 3: Time course of 5HT4R-T7-Rho$_{15}$ expression in mouse retina. (A) Immunostaining of 5HT4R-T7-Rho$_{15}$ in transgenic mouse retinas by T7 mAb. Shown from left to right are retinas of transgenic mice collected at 3−8 weeks of age and WT retinas at 8 weeks of age. Immunostaining reveals expression of 5HT4R-T7-Rho$_{15}$ (T7 mAb, red) in retinas of 5HT4R-T7-Rho$_{15}$ transgenic mice but not in the WT control. (B) Immunoblots of retinal extracts collected from the same mice shown in panel A, with T7 mAb used as the primary antibody. Immunoblots of anti-β-tubulin were used as internal controls. Lane M contains molecular weight markers. (C) Relative expression of 5HT4R-T7-Rho$_{15}$ as a function of age. Analyses were conducted by quantification of immunoblots with Bio-Rad QuantiOne as described in Materials and Methods.

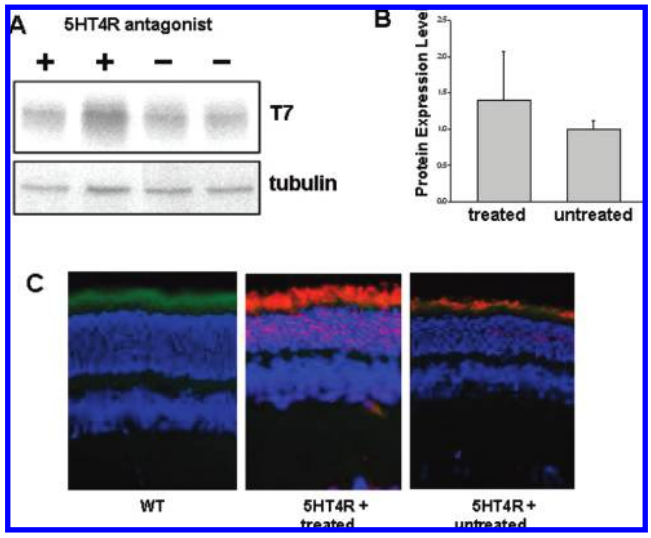

FIGURE 4: Effect of antagonist RS39604 treatment on expression of 5HT4R-T7-Rho$_{15}$ in transgenic mice. (A) Immunoblot analysis of 5HT4R-T7-Rho$_{15}$ expression levels. Lactating females with 1-week-old transgenic pups were provided drinking water containing 10 μM RS39604 for 2 weeks. Eyes and retinas were collected from 3-week-old pups in treated (+) and control (−) groups. (B) Quantification of receptor expression. Immunoblots were quantified with Bio-Rad QuantiOne as described in Materials and Methods. β-Tubulin immunoblots were used for normalization. The data are presented with the standard deviation. (C) Immunocytochemistry of receptor expression. Immunostaining revealed the expression of opsin (B6-30 mAb, green) in WT mice and 5HT4R-T7-Rho$_{15}$ expression (T7 mAb, red) in the retina of antagonist-treated and untreated transgenic mice. Nuclei were stained with DAPI (blue). The retina from a mouse treated with antagonist exhibited a higher level of expression of the receptor.

cryosections of mouse retina were rinsed in 10 mM phosphate (pH 7.4), 137 mM NaCl, and 2.7 mM KCl (PBS) and blocked with 10% goat serum in PBS. Either the B6-30 monoclonal antibody (mAb) (*21*) diluted 1:400 with PBS or the T7 mAb (Novagen) diluted 1:200 was used as the primary antibody. The B6-30 mAb, which recognizes the N-terminus of rhodopsin, was conjugated to Alexa 488 by use of the Alexa Fluor 488 Microscale Protein Labeling Kit (Invitrogen). Cy3-conjugated goat anti-mouse IgG (Jackson Immunoresearch Laboratories, West Grove, PA) diluted 1:200 with PBS was used as the secondary antibody. Nuclei were counterstained with 4′,6-diamidino-2-phenylindole (DAPI). Sections were analyzed with a Leica DM6000 B microscope. Digital images were captured with a RETIGA EXi FAST 1394 CCD camera (Q-Imaging Corp.).

SDS−PAGE Immunoblotting Analyses of Retinal Homogenates. Retinas from WT and transgenic mice (or comparable cell culture samples) were collected and homogenized in PBS with protease inhibitors using a Dounce homogenizer, solubilized in SDS sample buffer, and separated on a 10% SDS−PAGE gel. For immunoblotting, proteins were transferred from SDS−PAGE gels onto a PVDF membrane and probed with T7 mAb conjugated to alkaline phosphatase (AP), or a primary antibody followed by an AP-conjugated secondary antibody. Signals were visualized after treatment with BCIP/NBT color development substrate (Promega Corp., Madison, WI). In some experiments, samples were deglycosylated with peptide-N4-(acetyl-β-glucosaminyl)asparagine amidase (PNGase F) (New England Biolabs, Ipswich, MA) at 37 °C for 1 h before being loaded onto SDS−PAGE gels.

Quantification of signals for both immunoblots and silver-stained gels was carried out using a Gel Doc system (Bio-Rad, Hercules, CA) in conjunction with QuantiOne (Bio-Rad). Volume values (area × intensity of the bands) were

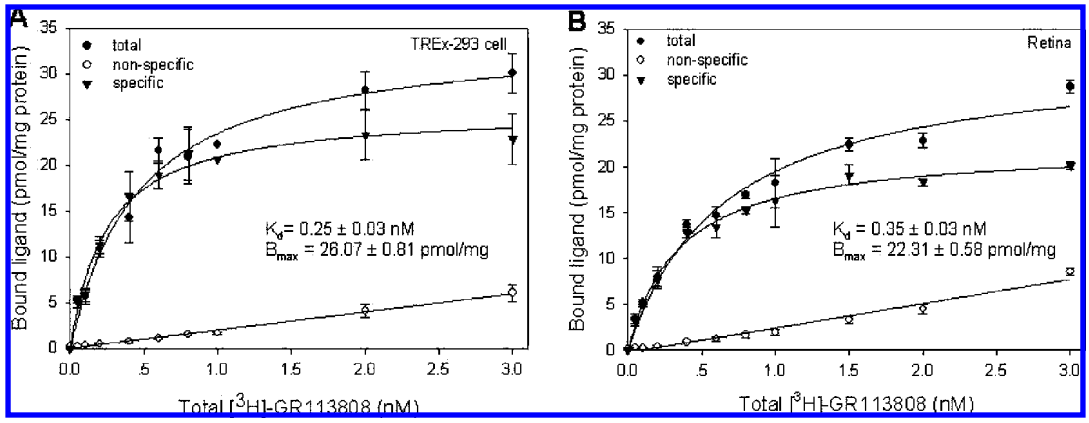

FIGURE 5: Saturation binding of antagonist GR113808 to 5HT4R-T7-Rho$_{15}$ expressed in TREx-293 cell membranes (A) and transgenic mouse retinal membranes (B). TREx-293 cell membranes and transgenic mouse retinal membranes were prepared as described in Materials and Methods. Membrane fractions were suspended in 25 mM HEPES (pH 7.4), 1 mM EDTA, and 2 mM $MgCl_2$ and incubated with increasing concentrations of [^{3}H]GR113808 (0−3 nM) in the presence of 0.5% BSA at 25 °C for 2 h with gentle shaking. Nonspecific binding was assessed by addition of 50 μM serotonin to the binding reaction mixture. Experiments were conducted in triplicate for each concentration point. The radioactivity of the bound ligand was measured as described in Materials and Methods. Data were fitted to one-site saturation binding curves with SigmaPlot version 10. The results indicate that the binding constants for binding of [^{3}H]GR113808 to 5HT4R-T7-Rho$_{15}$ expressed in TREx-293 cell membranes and transgenic mouse retinas are similar.

Table 1: Affinity Values of [^{3}H]GR113808 for 5HT4R-T7-Rho$_{15}$ from Various Sources

	TREx-293 cell		transgenic retina		
	a[a]	b[b]	a[a]	b[b]	purified receptor
K_d (nM)	0.25 ± 0.03	1.59 ± 0.49	0.35 ± 0.03	1.81 ± 0.40	1.03 ± 0.27

[a] Crude membrane. [b] Digitonin-solubilized membrane.

measured; the background was subtracted, and the results were normalized against internal controls.

Preparation of Membranes from TREx-293 Cells or Transgenic Mouse Retinas for Radioligand Binding Assays. Expression of 5HT4R-T7-Rho$_{15}$ in TREx-293 cells at 80% cellular confluence was induced by 1 μg/mL tetracycline for 24 h. Cells were then harvested by centrifugation at 200*g* for 5−10 min and subjected to hypotonic shock in lysis buffer [25 mM HEPES (pH 7.4), 2 mM benzamidine, and 0.2 mM PMSF] containing benzonase (Novagen). Suspensions were centrifuged at 20000*g* for 30 min, and membrane pellets were washed twice with lysis buffer before being aliquoted and stored at −80 °C for further use. Retinas from 5HT4R-T7-Rho$_{15}$ positive transgenic mice were obtained from 3-week-old animals, Dounce-homogenized in lysis buffer, and centrifuged at 20000*g* for 30 min. The resulting membrane pellets were washed twice with lysis buffer, aliquoted, and stored at −80 °C for further use.

Radioligand Binding Assays of Membrane-Bound Receptors. Membrane preparations equivalent to 0.5 × 10^6 TREx-293 cells or one transgenic mouse retina were suspended in each milliliter of binding buffer [25 mM HEPES (pH 7.4), 1 mM EDTA, and 2 mM $MgCl_2$]. For saturation binding studies, 20 μL of a membrane suspension was incubated with increasing concentrations of [^{3}H]GR113808 in binding buffer with 0.5% bovine serum albumin (BSA) at 25 °C for 2 h. Nonspecific binding was assessed by adding 50 μM serotonin to the binding reaction mixture. For competition binding studies, 20 μL of a membrane suspension was incubated with 0.25 nM [^{3}H]GR113808 and increasing concentrations of unlabeled agonist or antagonists in binding buffer with 0.5% BSA at 25 °C for 2 h. Total reaction volumes were 200 μL, and each binding reaction was conducted in triplicate. Binding reactions were stopped by fast filtration through a GF/B filter (Millipore), and the filter was washed three times with cold binding buffer. Washed GF/B filters were soaked in scintillation cocktail (Perkin-Elmer), and radioactivity was quantified with a LS 6500 scintillation counter (Beckman). Binding data were fitted in SigmaPlot version 10 either with a one-site saturation curve or with a one-site competition curve. For competition curves, EC_{50} values were derived by a nonlinear regression fit and transformed into K_i values with the Chang−Prussoff equation (*22*). Total membrane protein content was determined by the DC RC method (Bio-Rad) with membranes solubilized in *n*-dodecyl β-D-maltoside.

Radioligand Binding Assays of Detergent-Solubilized Receptors. To determine the ligand binding behavior of solubilized receptors (from either crude membrane extracts or immunoaffinity-purified preparations) in various detergents, we performed solution-based radioligand binding assays. Reaction mixtures totaling 50 μL containing solubilized receptors, 0.5% BSA, [^{3}H]GR113808, and the corresponding detergent were incubated at 25 °C for 1 h. They were then loaded onto 5 mL prepacked dextran desalting columns (Pierce) and eluted by gravity flow with cold binding buffer containing the same detergent. To determine the elution profile, we collected 18 × 0.5 mL fractions and added 5 mL of scintillation cocktail to each fraction. Radioactivity in each fraction was detected with a LS 6500 scintillation counter. All data analyses were carried out in the same manner as described for the membrane-based binding assays.

Purification of 5HT4R-T7-Rho$_{15}$. Eyes were harvested from 600 3-week-old offspring of transgenic × WT crossed mice and frozen. The entire harvest (1200 eyes) was suspended in 280 mL of 2 mM bis-tris-propane (BTP) (pH 7) and 2 mM EDTA with benzamidine and PMSF and homogenized first with a food processor and then with a Dounce glass homogenizer. The suspension was centrifuged for 30 min at 37000*g* at 4 °C, and the resulting membrane pellet was resuspended with a glass Dounce homogenizer in 470 mL of 50 mM Tris (pH 7.4), 280 mM NaCl, 6 mM KCl, and 2

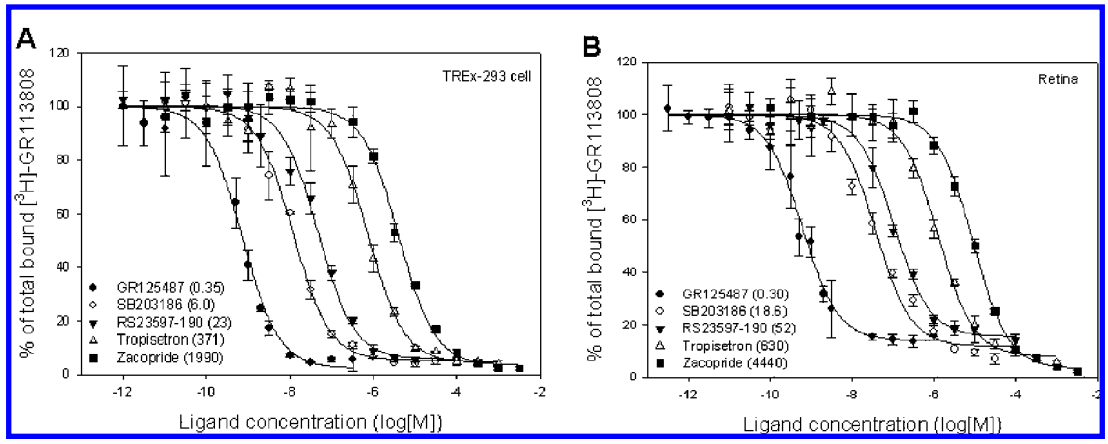

FIGURE 6: Competition between an agonist and antagonists with GR113808 for binding to 5HT4R-T7-Rho$_{15}$ expressed in TREx-293 cell membranes (A) and transgenic mouse retinal membranes (B). TREx-293 cell membranes and transgenic mouse retinal membranes, prepared as described in Materials and Methods, were suspended in 25 mM HEPES (pH 7.4), 1 mM EDTA, and 2 mM $MgCl_2$ and incubated with 0.25 nM [^{3}H]GR113808 and increasing concentrations of 5 unlabeled ligands in binding buffer containing 0.5% BSA at 25 °C for 2 h with gentle shaking. Experiments were conducted in triplicate for each concentration point. Radioactivity was detected as described in Materials and Methods. All data were fitted to one-site competition curves with SigmaPlot version 10; EC_{50} values were obtained, and K_i values were calculated according to the Cheng−Prusoff equation (*22*). Numbers in parentheses after each ligand named in the plots refer to the nanomolar K_i value for that ligand. 5HT4R-T7-Rho$_{15}$ expressed in either TREx-293 cell membranes or transgenic mouse retinas showed the same rank order of binding affinity for the tested ligands (GR125487 > SB201386 > RS23597-190 > Tropisetron > Zacopride).

Table 2: K_i Values of Various Ligands Displacing [^{3}H]GR113808 from 5HT4R-T7-Rho$_{15}$ from Various Sources

	K_i (nM) (log EC_{50}[a] ± standard error)		
	TREx-293 cell	retina	purified receptor
GR125487	0.25 (−9.14 ± 0.06)	0.35 (−9.22 ± 0.05)	1.79 (−8.27 ± 0.02)
SB203186	6 (−7.92 ± 0.04)	18.6 (−7.43 ± 0.08)	30.15 (−7.03 ± 0.11)
RS23597-190	23 (−7.33 ± 0.06)	52 (−6.98 ± 0.05)	440 (−5.88 ± 0.15)
Tropisetron	371 (−6.13 ± 0.07)	630 (−5.90 ± 0.06)	not determined
Zacopride	1990 (−5.40 ± 0.04)	4440 (−5.05 ± 0.03)	6960 (−4.67 ± 0.09)

[a] Log EC_{50} and standard errors were included because this is the real value that was fitted in the curve. K_i values were calculated from log EC_{50} values, and the standard errors were not provided since it is not proportional to the standard error of log EC_{50}.

mM EDTA (with benzamidine and PMSF). Membrane proteins were solubilized in digitonin at a final concentration of 1.6 mM for 30 min at 4 °C with gentle rocking. The sample was centrifuged for 30 min at 48000*g*, and 480 mL of crude extract was loaded onto a 0.5 cm diameter column containing 1 mL of T7 immunoaffinity agarose (Novagen) at a flow rate of 0.28 mL/min at 4 °C. The column was washed at 0.28 mL/min with 30 mL of 0.2 mM digitonin in 100 mM Tris (pH 7.4), 280 mM NaCl, and 6 mM KCl, and the receptor was eluted with 15 mL of ~1 mg/mL MASMTG-GQQMG peptide in the same buffer, at a flow rate of 23 μL/min. Samples were analyzed by SDS−PAGE, immunoblotting, and silver staining as described for the retinal homogenates, and radioligand binding assays.

For immunoblotting, 1D4 mAb or AP-conjugated T7 mAb was used as the primary antibody, and AP-conjugated rabbit anti-mouse IgG was used as the secondary antibody. Anti-C-terminal rhodopsin 1D4 mAb was purified by DEAE anion exchange chromatography and coupled to CNBr-activated Sepharose 4B (GE Healthcare) following the manufacturer's directions. Aliquots of the most enriched fractions were concentrated ~20 times with a Microcon YM-30 centrifugal device (Millipore) and used for the Coomassie-stained gel. The amount of purified receptor present was estimated by densitometry of silver-stained SDS−PAGE gels and by the Bradford colorimetric assay (*23*). The amount of material present in the silver-stained bands was quantified by using Bio-Rad QuantiOne, and the data were compared to a calibrated standard curve ($R^2 = 0.9965$, linear fit) generated with purified bovine rhodopsin (*24*). For the Bradford colorimetric dye binding procedure, 50 μL of each protein sample was mixed with 200 μL of Protein Assay Dye Reagent Concentrate (Bio-Rad) and 750 μL of water, and $A_{600} - A_{465}$ was measured after 40 min. In the case of the Bradford assay, standardized amounts of bovine serum albumin (BSA) were used to generate a calibration curve ($R^2 = 0.9754$, linear fit), and values for the eluted fractions were interpolated from it.

RESULTS

Engineering Transgenic Mice. The 5HT4R-T7-Rho$_{15}$ transgene construct consisted of five fragments: (1) a previously characterized mouse opsin promoter containing a 5 kb sequence upstream of the start codon (*25*), (2) a full-length human 5HT4bR coding sequence, and (3) a sequence encoding the initial 11 amino acids of the major capsid protein of T7 bacteriophage that is the epitope for the T7 mAb, followed by (4) a sequence encoding the 15-residue C-terminal region of mouse opsin containing the ROS-targeting signal with the epitope for the 1D4 mAb (*16*) and finally (5) an SV40 derived polyadenylation site (*26*) (Figure 1). Pronuclear injection of the 5HT4R-T7-Rho$_{15}$ transgene construct into FVB/N mice produced a total of five male transgenic founders. These positive males then were bred with C57BL/6J wild-type females to generate F1 animals.

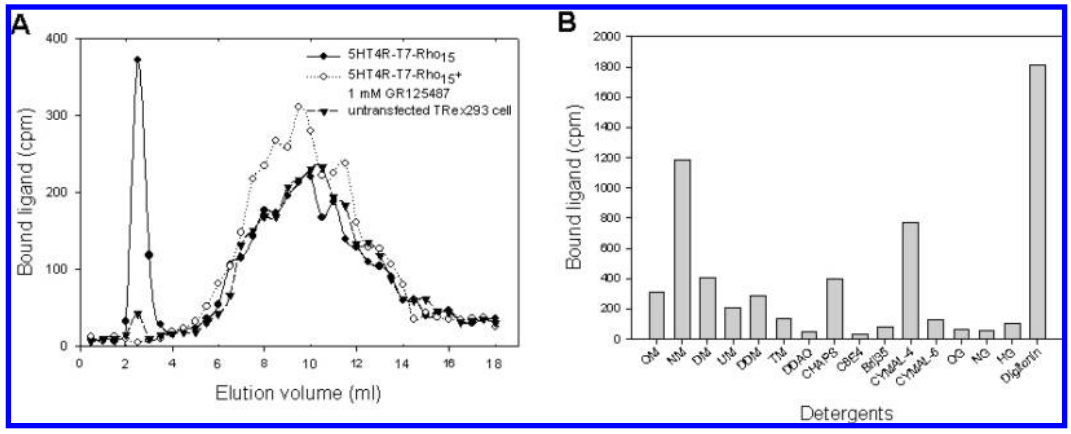

FIGURE 7: Ligand binding to detergent-solubilized 5HT4R-T7-Rho_{15}. Membranes from 2.8×10^6 5HT4R-T7-Rho_{15}-expressing TREx-293 cells were solubilized in 60 μL of detergent (0.5%) at 4 °C for 1 h. Solubilized receptors were clarified by high-speed centrifugation, and 5 μL of the crude supernatant was used for each ligand binding assay. Assays were carried out in 50 μL reaction mixtures containing solubilized sample, 0.5% BSA, 25 mM HEPES (pH 7.4), 1 mM EDTA, 2 mM $MgCl_2$, 2 nM [^{3}H]GR113808, and 0.5% solubilizing detergent at 25 °C for 1 h. Reactions were stopped by loading mixtures onto 5 mL prepacked dextran desalting columns eluted with a cold binding buffer containing 0.5% solubilizing detergent. Eighteen 0.5 mL fractions were collected from each column, and their radioactivity was measured. (A) Elution profile of a binding assay mixture from a dextran column (exemplified by NM-solubilized 5HT4R-T7-Rho_{15} as a solid line with filled circles) showing complete separation of bound (first peak) from free (second peak) radioligand. Untransfected TREx-293 cell membranes (dashed line with triangles) failed to bind [^{3}H]GR113808 under the same conditions. Addition of 1 mM unlabeled GR125487 totally ablated binding of [^{3}H]GR113808 to 5HT4R-T7-Rho_{15} in TREx-293 membranes (dotted line with empty circles). These results indicate that binding of [^{3}H]GR113808 to detergent-solubilized 5HT4R-T7-Rho_{15} is specific. (B) The area under the first peak representing bound radioligand is shown for each detergent-solubilized 5HT4R-T7-Rho_{15} binding assay. Digitonin provided the best binding activity of [^{3}H]GR113808 with respect to detergent-solubilized 5HT4R-T7-Rho_{15} of all detergents tested. Abbreviations: OM, *n*-octyl β-D-maltopyranoside; NM, *n*-nonyl β-D-maltopyranoside; DM, *n*-decyl β-D-maltopyranoside; UM, *n*-undecyl β-D-maltopyranoside; DDM, *n*-dodecyl β-D-maltopyranoside; TM, *n*-tetradecyl β-D-maltopyranoside; DDAO, *n*-dodecyl-*N*,*N*-dimethylamin-*N*-oxide; CHAPS, 3-[(3-cholamidopropyl)dimethylammonio]-1-propanesulfonate; C8E4, *n*-octyl tetraethylene glycol monoether; Brij35, polyoxyethylene 23 lauryl ether; CYMAL-4, cyclohexyl butyl-β-D-maltoside; CYMAL-6, cyclohexyl hexyl-β-D-maltoside; OG, *n*-octyl β-D-glucopyranoside; NG, *n*-nonyl β-D-glucopyranoside; HG, *n*-heptyl β-D-thioglucopyranoside.

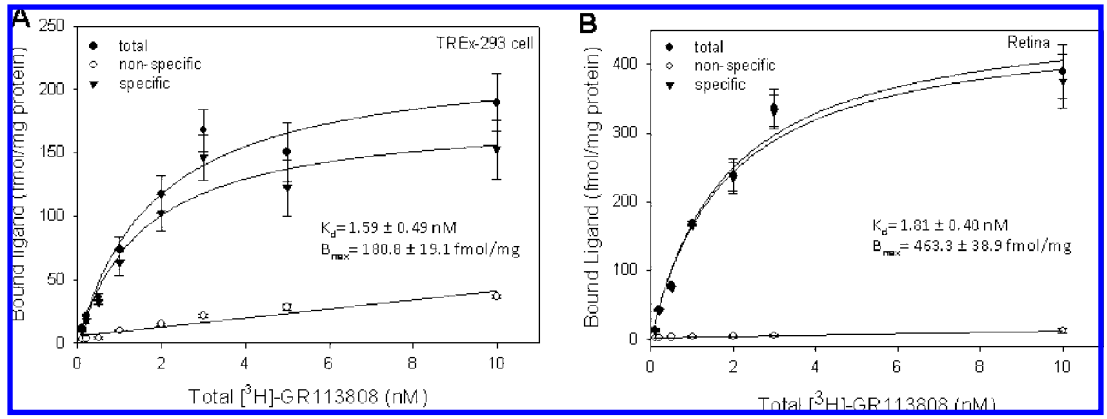

FIGURE 8: Saturation binding of GR113808 to digitonin-solubilized 5HT4R-T7-Rho_{15} expressed in either TREx-293 cell membranes (A) or transgenic mouse retinal membranes (B). TREx-293 membranes and transgenic mouse retinas were prepared as described in Materials and Methods. Cell membranes (100×10^6) or retinal membranes (20) were solubilized in 3.2 mM digitonin at 4 °C. Clarified solubilized crude supernatants were incubated with increasing concentrations of [^{3}H]GR113808 in 25 mM HEPES (pH 7.4), 1 mM EDTA, and 2 mM $MgCl_2$ containing 0.5% BSA and 3.2 mM digitonin at 25 °C for 1 h with gentle shaking. Total reaction volumes were 50 μL. Nonspecific binding was assessed by adding 1 mM serotonin to reaction mixtures. Experiments for each concentration point were conducted in triplicate. Bound and free radioligands were separated as described in Materials and Methods. The data were fitted to one-site saturation curves with SigmaPlot version 10. Binding affinities of [^{3}H]GR113808 for digitonin-solubilized 5HT4R-T7-Rho_{15} from TREx-293 cell membranes or transgenic mouse retinas are consistent with those obtained with homogenized native membrane-based binding assays.

Because FVB/N mice manifest the *rd* mutation that affects retinal morphology, we tested for the PDE6 genotype to screen out this mutation. Only 5HT4R-T7-Rho_{15} positive transgenic mice with a PDE6 WT background were used for subsequent studies.

Retinal Morphology and Receptor Localization. Retinas harvested from transgene positive F1 animals and WT littermates were tested for the presence of the 5HT4R-T7-Rho_{15} fusion protein by immunoblot analyses with T7 mAb. Animals were ranked on the basis of the intensity of the T7 signal which was taken as an indicator of total receptor fusion protein. F1 offspring from a particular 5HT4R-T7-Rho_{15} transgenic founder (F1976) showed the highest expression level of total receptor protein by this criterion (comparative data not shown). This transgenic mouse line was then examined for retinal morphology by DAPI staining. Inspection of retinal sections from F1976-derived F1 offspring at the age of 4 weeks revealed that 5HT4R-T7-Rho_{15} expression was most prominent in the ROS layer with lower levels manifest in both the outer nuclear layer (ONL) and inner

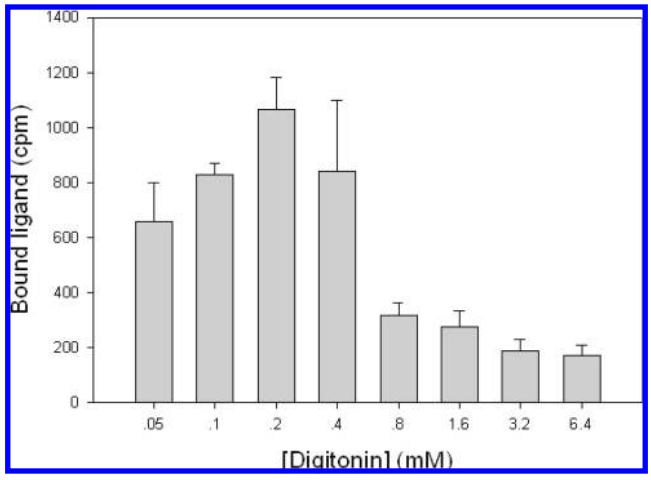

FIGURE 9: Effect of digitonin concentration on ligand binding of immunoaffinity-purified 5HT4R-T7-Rho$_{15}$. TREx-293 cell membranes from 300 × 10^6 cells expressing 5HT4R-T7-Rho$_{15}$ were solubilized in 9 mL of 3.2 mM digitonin buffer. The clarified crude extract was incubated with 0.5 mL of pre-equilibrated 1D4 immunoaffinity agarose beads for 1 h at 4 °C with gentle shaking. 1D4 immunoaffinity beads with bound protein then were divided into eight equal portions. Each portion was washed with buffers containing a different concentration of digitonin. The receptor was eluted with 1 mg/mL competing peptide in the same washing buffer. Identical amounts of eluate from each 1D4 immunoaffinity batch of beads were incubated with 2 nM [^{3}H]GR113808 in 25 mM HEPES (pH 7.4), 1 mM EDTA, and 2 mM $MgCl_2$ containing 0.5% BSA and the shown concentration of digitonin for 1 h at 25 °C. Each reaction was carried out in triplicate. The bound radioligand peak from each dextran column was collected, and its radioactivity was plotted vs the concentration of digitonin used for the washing, eluting, and binding steps. The results show that elution with 0.2 mM digitonin provided optimal ligand binding activity of purified 5HT4R-T7-Rho$_{15}$.

segment (IS) by immunocytochemistry (Figure 2). Using a B6-30 mAb probe, opsin could be localized in the ONL of both WT and transgenic mice which also appeared to contain similar numbers of nuclei as indicated by DAPI staining (Figure 2).

Optimal Age for Harvesting Transgenic Retinas. Retinas of mice at different ages were harvested and analyzed for fusion protein expression by immunocytochemistry (Figure 3A) and immunoblotting (Figure 3B,C). Maximal expression assessed by immunoblotting was observed in 3-week-old mice, an age at which retinas are well developed in WT animals (*27*). On the basis of these observations, retinas from 3-week-old transgenic and WT control mice were used for all subsequent studies.

Effect of Antagonist on the Expression of 5HT4R-T7-Rho$_{15}$ in Transgenic Mice. Several previous studies with heterologous expression systems indicated that the level of GPCR expression can be increased by the presence of antagonists (*28*). To study the effect of a 5HT4R antagonist on transgenic expression and stability of retinal structures, we fed 1-week-old transgenic pups indirectly via their lactating mothers with 10 μM RS39604 in the parental drinking water. After being exposed for 2 weeks, retinas were harvested from the pups for immunoblotting (Figure 4A,B) and immunocytochemistry (Figure 4C). Immunoblot signals were normalized against a β-tubulin internal control for quantification (Figure 4B). The results indicate that antagonist treatment under these conditions slightly improved expression levels of the target receptor and the morphology of the ROS in these mice.

Pharmacology of 5HT4R-T7-Rho$_{15}$. To evaluate the pharmacological activity of 5HT4R-T7-Rho$_{15}$ expressed in transgenic mouse retina, we performed radioligand binding assays on transgene positive retinal membranes and compared the results with those of identical receptors expressed in the membranes of cultured mammalian cells. Saturation binding with increasing concentrations of [^{3}H]GR113808 in membrane preparations of transgenic mouse retinas or transfected TREx-293 cell membranes yielded similar binding affinities for GR113808 (Figure 5 and Table 1). Competitive displacement of the radioligand with five 5HT4R specific ligands also showed the same rank order of potency in both types of membranes: GR125487 > SB201386 > RS23597-190 > Tropisetron > Zacopride (Figure 6 and Table 2). The binding affinities of tested ligands for both tissues are consistent with previously reported values (*29*−*31*). These results indicate that the receptor expressed in our transgenic mouse retina expressing system exhibits proper ligand binding activity and therefore should be properly folded.

Effects of Different Detergents on Ligand Binding by 5HT4R-T7-Rho$_{15}$. Various detergents were tested for their ability to solubilize the receptor and maintain its ligand binding activity. Separation of bound and free radioligand in these solution-based binding assays was achieved by gel filtration (*32*). As illustrated by Figure 7A for one of the examined detergents, 0.5% *n*-nonyl β-D-maltopyranoside, a 5 mL prepacked dextran desalting column successfully segregated receptor-bound from free radioligand. Among all the mild detergents tested, digitonin best preserved the binding activity of the solubilized receptor (Figure 7B).

To further evaluate the ability of digitonin to stabilize the receptor, we performed ligand saturation binding assays with increasing concentrations of [^{3}H]GR113808 at a fixed concentration of digitonin-solubilized receptor. As shown in Figure 8, 5HT4R-T7-Rho$_{15}$ expressed in either TREx-293 cell membranes or transgenic mouse retinas and solubilized in 3.2 mM digitonin exhibited similar binding activities and affinities for [^{3}H]GR113808 (Table 1). These results indicate that the receptor from both tissue sources had a similar response to solubilization by digitonin and, most importantly, maintained a conformation sufficient for specific recognition of the receptor's antagonist.

To determine the optimal concentration of digitonin needed to maintain ligand recognition in a purified form, we isolated the purified 5HT4R-T7-Rho$_{15}$ by 1D4 affinity batch purification and assayed its ligand binding activity in the presence of various concentrations of digitonin. Figure 9 shows that 0.2 mM digitonin provided the best level of binding for the solubilized and delipidated receptor. In a similar manner, the optimal digitonin concentration during membrane solubilization was determined to be 1.6 mM (not shown).

Purification of GPCR-T7-Rho$_{15}$ from Transgenic Mice. A general protocol for purifying T7-Rho$_{15}$-tagged GPCRs coexpressed with rhodopsin in rod cells of transgenic mice and partially optimized for 5HT4R-T7-Rho$_{15}$ was developed (Figure 10). The parent heterozygote breeding stock used to produce animals for purification experiments was expected to produce offspring that were 50% positive for the 5HT4R-T7-Rho$_{15}$ transgene and 50% WT. No attempt was made to segregate positive eyes from WT eyes during the harvest. A total of 1200 eyes (from 600 mixed population offspring) were used to prepare a digitonin-solubilized membrane

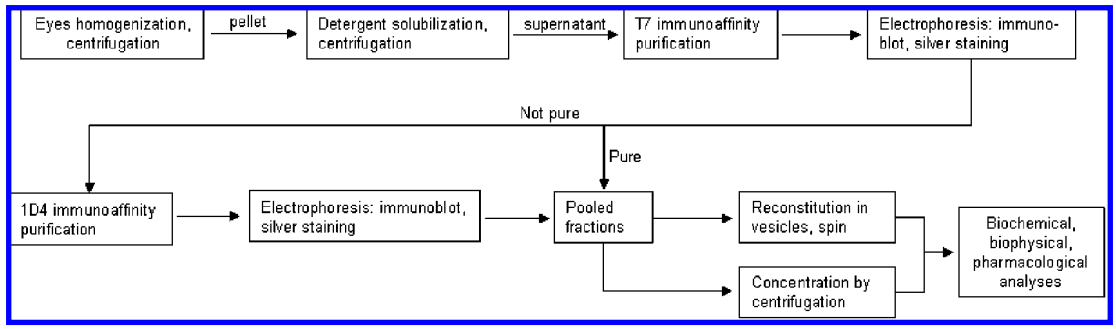

FIGURE 10: Flowchart for purification of 5HT4R-T7-Rho$_{15}$ from transgenic mice. Frozen mouse eyes were homogenized with 2 mM BTP (pH 7.0) containing 2 mM EDTA and protease inhibitors. Soluble fractions were discarded, and 5HT4R-T7-Rho$_{15}$ was extracted from membrane pellets with Tris saline (pH 7.4) containing 3.2 mM digitonin. The receptor was purified by T7 immunoaffinity chromatography as described in Materials and Methods. Purity and activity were assessed by SDS−PAGE, immunoblotting, and radioligand binding assays. For some experiments, the receptor was rechromatographed on a 1D4 immunoaffinity column, concentrated, and analyzed as described in Materials and Methods.

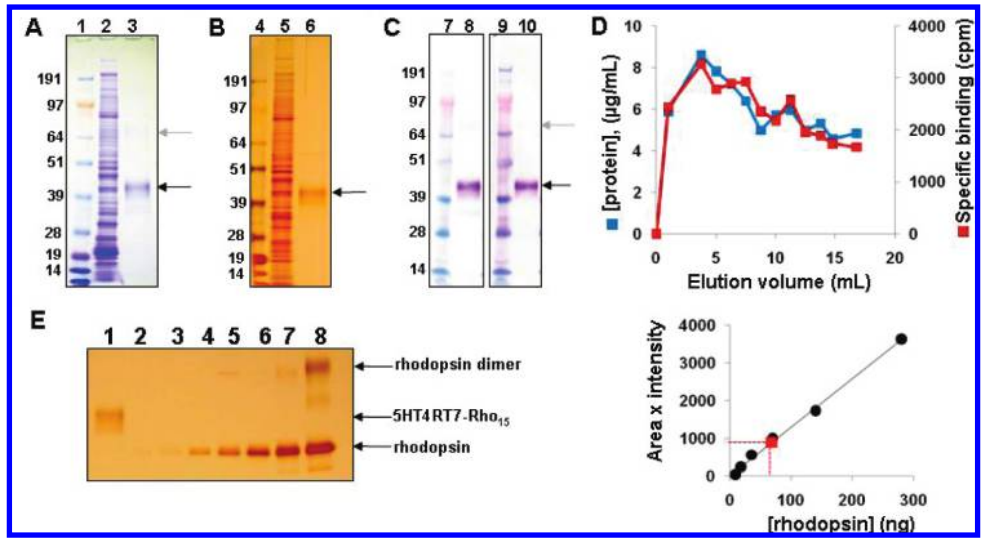

FIGURE 11: Purification of 5HT4R-T7-Rho$_{15}$ by T7 immunoaffinity chromatography. (A) Coomassie-stained SDS−PAGE gel showing a digitonin-solubilized membrane protein fraction from mixed transgenic and WT mouse eyes (lane 2) and purified receptor (lane 3). Purified samples were concentrated ~20-fold with a Microcon YM-30 centrifugal device. (B) Silver-stained SDS−PAGE gel showing a digitonin-solublized membrane protein fraction (lane 5) and purified receptor (lane 6). (C) Immunoblots of purified receptor probed with 1D4 mAb (lane 8) and alkaline phosphatase-conjugated T7 mAb (lane 10). Lanes 1, 4, 7, and 9 contained markers with known molecular masses shown at the left. Black arrows indicate the bands corresponding to the receptor monomer and gray arrows faint dimer bands. (D) Chromatographic profiles monitored by protein concentration (determined by Bradford colorimetric assay, blue squares) and specific radioligand binding (red squares). (E) Quantification of the purified receptor by densitometric analysis of a silver-stained SDS−PAGE gel. In the gel, lane 1 corresponds to 10.5 μL of pooled elution fractions (total volume of 15 mL) whereas lanes 2−8 contained increasing amounts of immunopurified bovine rhodopsin. The plot at the right shows the intensity × area of the bands for different amounts of rhodopsin (●) and the interpolated value for the band of purified 5HT4R-T7-Rho$_{15}$ in lane 1 (red square).

fraction which was then loaded onto a 1 mL T7 immunoaffinity column and washed with 30 column volumes of buffer before the purified receptor was eluted with competing T7 peptide. The crude extract contained a very complex mixture of proteins (Figure 11A,B, lanes 2 and 5) that was reduced to a single species during the single chromatographic step (Figure 11A,B, lanes 3 and 6). The identity of this species as the receptor fusion protein was verified by immunoblotting with T7 and 1D4 mAbs (Figure 11C, lanes 8 and 10, respectively). The elution fractions showed a good correlation between protein content [estimated by Bradford's colorimetric assay (*23*)] and 5HT4R binding activity (estimated by a solution-based radioligand binding assay) (Figure 11D), demonstrating that the fractions actually contained purified functional receptor. The total amount of eluted receptor was also estimated by densitometric analysis of silver-stained SDS−PAGE gels with purified rhodopsin used as the standard (Figure 11E). Both the Bradford assay and gel analysis provided a similar estimate that 90−107 μg of 5HT4R-T7-Rho$_{15}$ was recovered in the total combined eluate. An accounting of the chromatography step revealed that during the initial loading of the affinity column approximately 55% of the binding activity present in the original solubilized extract had been lost, most likely do to exceeding the capacity of the column and/or slow T7 tag−antibody binding kinetics (data not shown). This suggests that with a larger capacity column it should be possible to increase the yield to ~200−300 μg of purified receptor from the same starting number of heterozygous mixed offspring.

Pharmacology of Purified 5HT4R-T7-Rho$_{15}$. Purified 5HT4R-T7-Rho$_{15}$ protein from the T7 immunoaffinity column in digitonin was nearly homogeneous as shown by silver-stained SDS−PAGE gels and immunoblotting (Figure 11). To assess the conformational state of the receptor, we performed solution-based radioligand binding assays. Saturation binding results revealed a binding affinity of GR113808 for the

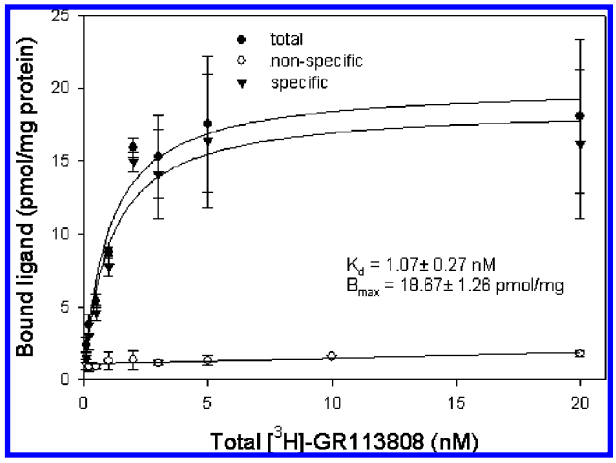

FIGURE 12: Saturation binding of GR113808 to immunoaffinity-purified 5HT4R-T7-Rho_{15} in digitonin. 5HT4R-T7-Rho_{15} expressed in transgenic mouse retinas was purified by T7 immunoaffinity chromatography as described in Materials and Methods. Purified receptor samples were incubated with increasing concentrations of [^{3}H]GR113808 in binding buffer [25 mM HEPES (pH 7.4), 1 mM EDTA, and 2 mM $MgCl_2$] containing 0.5% BSA and 0.2 mM digitonin at 25 °C for 1 h. Experiments for each concentration point were conducted in triplicate. Nonspecific binding was assessed by addition of 1 mM serotonin to the reaction mixture. The bound radioligand peak was collected from each dextran column and its radioactivity counted. Data were fitted to one-site saturation binding curves with SigmaPlot version 10. Purified 5HT4R-T7-Rho_{15} had an affinity for [^{3}H]GR113808 similar to that of crude retinal membranes extracted with digitonin.

purified receptor similar to that found with crude membranes extracted with digitonin (Figure 12 and Table 1). Furthermore, competition binding with four ligands showed not only that the rank order displacement of these four ligands with the purified receptor was the same as in the membrane-based assays but also that the affinities of these ligands were in the same range as well (Figure 13).

DISCUSSION

Although heterologous expression of integral membrane proteins is common practice, the biosynthesis and isolation of such proteins from conventional prokaryotic or eukaryotic expression systems in a form suitable for biophysical studies have proven to be difficult. For example, GPCRs overexpressed in bacteria lack post-translational modifications and often need to be refolded from inclusion bodies (*33*), a procedure that is difficult for proteins containing discontinuous stretches of α-helical sequences (*34, 35*). Mammalian cell and unicellular eukaryotic expression systems (*36*−*38*), cell-free systems (*39*), and even transgenic mouse liver (*12*) are also capable of generating GPCR protein, but the protein produced generally proves refractory to crystallization. While the exact nature of these systems' deficits is debatable, their shortcomings with regard to crystallization trials include unpredictable and often low levels of expression along with the incorporation of non-native nonuniform post-translational modifications.

The challenge posed by low overall receptor protein content is daunting but can be overcome if one is willing to accept the expense associated with increasing the scale of the system. Aberrant post-translational processing, however, presents a more fundamental problem. Strategies that employ extensive sequence modifications, including interruption of the receptor backbone by introduction of extraneous extramembrane domains to stabilize post-translational folding, have recently yielded GPCR crystals (reviewed in ref *3*). However, the relevance of crystals generated from such mutant protein constructs for the study of native receptor function could be viewed as compromised. The matter of glycosylation is also important, and a common tactic used to reduce this source of potential structural heterogeneity is the simple recombinant removal of all possible glycosylation sites. While some normally glycosylated proteins function perfectly well without their sugars, others do not fare as well, their glycosylation state being crucial for correct protein folding and/or membrane insertion and transport (*40, 41*). It has also been shown that carbohydrates can be involved in crystal contacts and therefore required for crystallization, but only if glycosylation is uniform and homogeneous (*24*).

For the reasons described above, we wish to develop a new in vivo expression system that has the potential to produce a concentrated source of GPCR protein which is homogeneously processed by a strictly controlled natural mammalian biosynthetic apparatus. On the basis of our previous experience purifying rhodopsin from retinal ROS and our understanding of the biosynthetic machinery in rod cells, we have attempted to usurp the ROS for the production of heterologous GPCR proteins.

Our initial attempts to completely replace endogenous retinal rhodopsin with a heterologous GPCR in a rhodopsin knockout background were unsuccessful, supporting the concept that rhodopsin serves as an essential component for retinal integrity which cannot be supplanted by even a structurally similar GPCR family member. Further work in which a heterologous GPCR (i.e., AA1R) was coexpressed along with rhodopsin proved more fruitful (*12*). The 5HT4R studies reported here build upon this work to achieve higher levels of receptor expression and to produce protocols for isolation of the receptors.

As with our previous work on AA1R, we find that the use of an opsin promoter in conjunction with the six- to eight-amino acid ROS targeting sequence is effective in generating transgenic mice that transport the 5HT4R-T7-Rho_{15} fusion protein to the ROS of their retinas. Our time course experiments in mice reveal that the expression of 5HT4R-T7-Rho_{15} peaked at 3 weeks of age (post natal), coinciding with maturation of the retina and ROS. A significant decline in both the level of 5HT4R expression and retinal structure ensued shortly thereafter. This is not surprising since it has been shown that disturbing the expression/transport system of rhodopsin inevitably causes some degree of retinal degeneration (*42*). Intriguing preliminary results showed that treatment with an antagonist can increase the level of expression of the target receptor (Figure 4). Similar "pharmacological chaperones" have been described for misfolded mutant receptors where ligand binding stabilized a properly folded conformation and increased the level of receptor expression (*43, 44*).

Our study of membrane fractions prepared from transgenic 5HT4R retinas reveals a pharmacological profile for 5HT4R similar to that of an analogous 5HT4R membrane preparation from a conventional cell culture system. Both the absolute affinity for the 5HT4R antagonist [^{3}H]GR113808 and the rank order potency for displacement of ligands diagnostic

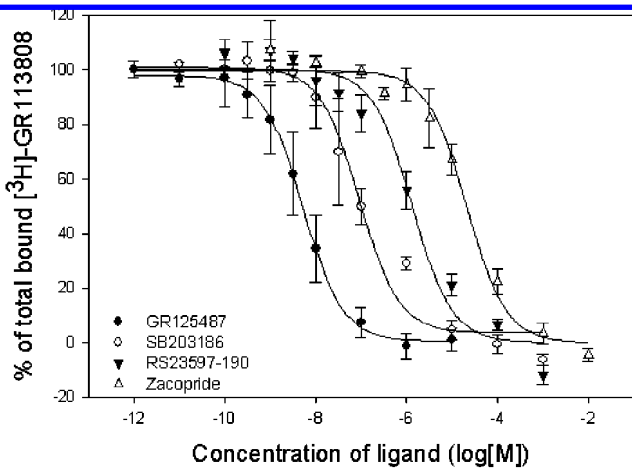

	GR125487	SB203186	RS23597-190	Zacopride
K_i (nM)	1.79	30.15	440	6960

FIGURE 13: Competition between an agonist and antagonists with GR113808 for binding to immunoaffinity-purified 5HT4R-T7-Rho_{15} in digitonin. 5HT4R-T7-Rho_{15} expressed in transgenic mouse retinas was purified by T7 immunoaffinity chromatography as described in Materials and Methods. Purified receptor samples were incubated with 2 nM [^{3}H]GR113808 and increasing concentrations of four unlabeled ligands in 25 mM HEPES (pH 7.4), 1 mM EDTA, and 2 mM $MgCl_2$ containing 0.5% BSA and 0.2 mM digitonin at 25 °C for 1 h. Each experiment at a given ligand concentration was conducted in triplicate. The bound radioligand peak was collected from a dextran column and its radioactivity counted. All data analyses and curve fitting were done with SigmaPlot version 10. K_i values were calculated as described previously. The K_i rank order of binding to purified 5HT4R-T7-Rho_{15} (shown in the table) was the same as that found for native membrane preparations.

of 5HT4R pharmacology indicate that the receptor is correctly folded in the transgenic retina.

As part of our work to enable crystallization, we investigated various methods for purifying the receptor. Solubilization is a prerequisite for such purification, and determining which detergent conditions best preserved the receptor's pharmacological conformation was approached empirically.

Some proteins, e.g., Na,K-ATPase (*45, 46*) or the cytochrome b_6f complex (*47*), cannot withstand complete delipidation and disaggregation without loss of enzyme activity, and we feared that it would be difficult to preserve receptor function after the delipidation expected to occur during our planned chromatographic purification. For this reason, we included digitonin in our survey of receptor solubilizing reagents with the hope that it could preserve an annulus of lipid sufficient to retain the core structure of the receptor protein. This detergent is commonly used to solubilize membrane proteins for biophysical studies because of its mild nature (*48*). Encouragingly, we also found that digitonin, as compared to other detergents, best preserved ligand binding activity after receptor solubilization and after subsequent chromatographic delipidation.

Subsequent purification of digitonin-solubilized 5HT4R-T7-Rho_{15} through T7 immunoaffinity chromatography was straightforward and produced a final preparation that appears essentially homogeneous by SDS−PAGE analysis. This one-step process significantly reduces the time the receptor is exposed to possible denaturing conditions and reduces the protein loss that might result from procedures requiring extra manipulation. Biochemical and pharmacological characterization of the purified delipidated receptor preparation indicates a good correlation between ligand binding activity and protein content, supporting the conclusion that the bulk of the protein produced by the protocol is composed of the active receptor species. The pharmacological profile of the purified protein faithfully displays the expected antagonist properties for 5HT4R. Previously reported work indicates that the rod cells are capable of producing adenosine A1R protein that is homogeneously glycosylated (*9*), and our preliminary observations suggest this is also the case with 5HT4R. Additional work is being done to confirm this and characterize the specific carbohydrate content of purified 5HT4R.

The purification protocol produced an overall yield of ~100 ng of pure receptor protein per eye as harvested from animals bred from a heterozygous line where ~50% of the harvested mice were WT. As mentioned above, optimizing the immunoaffinity column protocol should double or triple this yield, while incorporation of genotyping into the harvest procedure to remove the non-5HT4R-expressing eye tissue should provide an additional 2-fold improvement and push the yield upward toward ~400−600 ng per eye with the current heterozygotic breeding line. We believe that additional efforts to produce improved homozygote lines and/or further improvements in our extraction−purification protocol could produce a yield approaching ~1 μg of purified receptor protein per transgenic mouse.

To be useful for crystallization (or other biophysical) studies, the purified protein must be sufficiently concentrated. Work to optimize the use of centrifugal concentrators, ultracentrifugation methods, and/or an additional 1D4 immunoaffinity step directed against the fused Rho_{15} tag to achieve higher receptor concentrations without concomitantly increasing the concentration of detergents or salts is currently ongoing.

In summary, we have demonstrated the feasibility of engineering transgenic mice that heterologously express 5HT4R in the retina's rod cells and that the resulting receptor

is present in a pharmacologically relevant conformation. A purification procedure has been developed that results in essentially pure and pharmacologically active protein that should be suitable for crystallization trials. Further optimization of the expression constructs with regard to promoter, polyadenylation signal, regulatory elements (including the use of inducible systems), and generation of new genetic strains of mice is ongoing and should further establish the ability of the ROS organelle to serve as a depot for 5HT4R and other GPCR proteins. In the meantime, recent advances in microfluidic crystallization methods and brighter, microfocused beam sources available for X-ray diffraction studies should allow us to take maximal advantage of the described 5HT4R receptor protein produced by the methods reported herein.

ACKNOWLEDGMENT

We thank Dr. Ning Li and the Transgenic and Targeting Facility at Case Western Reserve University for assistance in developing some of the transgenic lines used in this study and Dr. William Harte, Dr. Joseph Jankowski, and Vida Tripodo for their support and critical discussions of this work.

REFERENCES

1. Kroeze, W. K., Sheffler, D. J., and Roth, B. L. (2003) G-protein-coupled receptors at a glance. *J. Cell Sci. 116*, 4867–4869.
2. Armbruster, B. N., and Roth, B. L. (2005) Mining the receptorome. *J. Biol. Chem. 280*, 5129–5132.
3. Mustafi, D., and Palczewski, K. (2008) Topology of class A G protein-coupled receptors: Insights gained from crystal structures of rhodopsins, adrenergic and adenosine receptors. *Mol. Pharmacol.* (in press).
4. Okada, T., Takeda, K., and Kouyama, T. (1998) Highly selective separation of rhodopsin from bovine rod outer segment membranes using combination of divalent cation and alkyl(thio)glucoside. *Photochem. Photobiol. 67*, 495–499.
5. Okada, T., Le Trong, I., Fox, B. A., Behnke, C. A., Stenkamp, R. E., and Palczewski, K. (2000) X-ray diffraction analysis of three-dimensional crystals of bovine rhodopsin obtained from mixed micelles. *J. Struct. Biol. 130*, 73–80.
6. Teller, D. C., Okada, T., Behnke, C. A., Palczewski, K., and Stenkamp, R. E. (2001) Advances in determination of a high-resolution three-dimensional structure of rhodopsin, a model of G-protein-coupled receptors (GPCRs). *Biochemistry 40*, 7761–7772.
7. Palczewski, K., Kumasaka, T., Hori, T., Behnke, C. A., Motoshima, H., Fox, B. A., Le Trong, I., Teller, D. C., Okada, T., Stenkamp, R. E., Yamamoto, M., and Miyano, M. (2000) Crystal structure of rhodopsin: A G protein-coupled receptor. *Science 289*, 739–745.
8. Palczewski, K. (2006) G protein-coupled receptor rhodopsin. *Annu. Rev. Biochem. 75*, 743–767.
9. Zhang, L., Salom, D., He, J., Okun, A., Ballesteros, J., Palczewski, K., and Li, N. (2005) Expression of Functional G Protein-Coupled Receptors in Photoreceptors of Transgenic *Xenopus laevis*. *Biochemistry 44*, 14509–14518.
10. Panneels, V., Eroglu, C., Cronet, P., and Sinning, I. (2003) Pharmacological characterization and immunoaffinity purification of metabotropic glutamate receptor from *Drosophila* overexpressed in Sf9 cells. *Protein Expression Purif. 30*, 275–282.
11. Eroglu, C., Cronet, P., Panneels, V., Beaufils, P., and Sinning, I. (2002) Functional reconstitution of purified metabotropic glutamate receptor expressed in the fly eye. *EMBO Rep. 3*, 491–496.
12. Li, N., Salom, D., Zhang, L., Harris, T., Ballesteros, J. A., Golczak, M., Jastrzebska, B., Palczewski, K., Kurahara, C., Juan, T., Jordan, S., and Salon, J. A. (2007) Heterologous expression of the adenosine A1 receptor in transgenic mouse retina. *Biochemistry 46*, 8350–8359.
13. Lem, J., Applebury, M. L., Falk, J. D., Flannery, J. G., and Simon, M. I. (1991) Tissue-specific and developmental regulation of rod opsin chimeric genes in transgenic mice. *Neuron 6*, 201–210.
14. Zack, D. J., Bennett, J., Wang, Y., Davenport, C., Klaunberg, B., Gearhart, J., and Nathans, J. (1991) Unusual topography of bovine rhodopsin promoter-lacZ fusion gene expression in transgenic mouse retinas. *Neuron 6*, 187–199.
15. al-Ubaidi, M. R., Pittler, S. J., Champagne, M. S., Triantafyllos, J. T., McGinnis, J. F., and Baehr, W. (1990) Mouse opsin. Gene structure and molecular basis of multiple transcripts. *J. Biol. Chem. 265*, 20563–20569.
16. MacKenzie, D., Arendt, A., Hargrave, P., McDowell, J. H., and Molday, R. S. (1984) Localization of binding sites for carboxyl terminal specific anti-rhodopsin monoclonal antibodies using synthetic peptides. *Biochemistry 23*, 6544–6549.
17. Kashanchi, F., Thompson, J., Sadaie, M. R., Doniger, J., Duvall, J., Brady, J. N., and Rosenthal, L. J. (1994) Transcriptional activation of minimal HIV-1 promoter by ORF-1 protein expressed from the SalI-L fragment of human herpesvirus 6. *Virology 201*, 95–106.
18. Batten, M. L., Imanishi, Y., Maeda, T., Tu, D. C., Moise, A. R., Bronson, D., Possin, D., Van Gelder, R. N., Baehr, W., and Palczewski, K. (2004) Lecithin-retinol acyltransferase is essential for accumulation of all-trans-retinyl esters in the eye and in the liver. *J. Biol. Chem. 279*, 10422–10432.
19. Maeda, A., Maeda, T., Imanishi, Y., Kuksa, V., Alekseev, A., Bronson, J. D., Zhang, H., Zhu, L., Sun, W., Saperstein, D. A., Rieke, F., Baehr, W., and Palczewski, K. (2005) Role of photoreceptor-specific retinol dehydrogenase in the retinoid cycle in vivo. *J. Biol. Chem. 280*, 18822–18832.
20. Imanishi, Y., Batten, M. L., Piston, D. W., Baehr, W., and Palczewski, K. (2004) Noninvasive two-photon imaging reveals retinyl ester storage structures in the eye. *J. Cell Biol. 164*, 373–383.
21. Adamus, G., Zam, Z. S., Arendt, A., Palczewski, K., McDowell, J. H., and Hargrave, P. A. (1991) Anti-rhodopsin monoclonal antibodies of defined specificity: Characterization and application. *Vision Res. 31*, 17–31.
22. Cheng, Y., and Prusoff, W. H. (1973) Relationship between the inhibition constant (K1) and the concentration of inhibitor which causes 50% inhibition (I50) of an enzymatic reaction. *Biochem. Pharmacol. 22*, 3099–3108.
23. Bradford, M. M. (1976) A rapid and sensitive method for the quantitation of microgram quantities of protein utilizing the principle of protein-dye binding. *Anal. Biochem. 72*, 248–254.
24. Salom, D., Lodowski, D. T., Stenkamp, R. E., Le Trong, I., Golczak, M., Jastrzebska, B., Harris, T., Ballesteros, J. A., and Palczewski, K. (2006) Crystal structure of a photoactivated deprotonated intermediate of rhodopsin. *Proc. Natl. Acad. Sci. U.S.A. 103*, 16123–16128.
25. Chen, J., Makino, C. L., Peachey, N. S., Baylor, D. A., and Simon, M. I. (1995) Mechanisms of rhodopsin inactivation in vivo as revealed by a COOH-terminal truncation mutant. *Science 267*, 374–377.
26. Breathnach, R., and Harris, B. A. (1983) Plasmids for the cloning and expression of full-length double-stranded cDNAs under control of the SV40 early or late gene promoter. *Nucleic Acids Res. 11*, 7119–7136.
27. Palczewski, K., Farber, D. B., and Hargrave, P. A. (1991) Elevated level of protein phosphatase 2A activity in retinas of rd mice. *Exp. Eye Res. 53*, 101–105.
28. Labrecque, J., Fargin, A., Bouvier, M., Chidiac, P., and Dennis, M. (1995) Serotonergic antagonists differentially inhibit spontaneous activity and decrease ligand binding capacity of the rat 5-hydroxytryptamine type 2C receptor in Sf9 cells. *Mol. Pharmacol. 48*, 150–159.
29. Eglen, R. M., Wong, E. H., Dumuis, A., and Bockaert, J. (1995) Central 5-HT4 receptors. *Trends Pharmacol. Sci. 16*, 391–398.
30. McLean, P. G., and Coupar, I. M. (1995) 5-HT4 receptor antagonist affinities of SB207710, SB205008, and SB203186 in the human colon, rat oesophagus, and guinea-pig ileum peristaltic reflex. *Naunyn-Schmiedeberg's Arch. Pharmacol. 352*, 132–140.
31. Van den Wyngaert, I., Gommeren, W., Verhasselt, P., Jurzak, M., Leysen, J., Luyten, W., and Bender, E. (1997) Cloning and expression of a human serotonin 5-HT4 receptor cDNA. *J. Neurochem. 69*, 1810–1819.
32. Park, P. S., Sum, C. S., Pawagi, A. B., and Wells, J. W. (2002) Cooperativity and oligomeric status of cardiac muscarinic cholinergic receptors. *Biochemistry 41*, 5588–5604.
33. Lundstrom, K. (2005) The future of G protein-coupled receptors as targets in drug discovery. *IDrugs 8*, 909–913.

34. Geertsma, E. R., Nik Mahmood, N. A., Schuurman-Wolters, G. K., and Poolman, B. (2008) Membrane reconstitution of ABC transporters and assays of translocator function. *Nat. Protoc. 3*, 256–266.
35. Geertsma, E. R., Groeneveld, M., Slotboom, D. J., and Poolman, B. (2008) Quality control of overexpressed membrane proteins. *Proc. Natl. Acad. Sci. U.S.A. 105*, 5722–5727.
36. Cherezov, V., Rosenbaum, D. M., Hanson, M. A., Rasmussen, S. G., Thian, F. S., Kobilka, T. S., Choi, H. J., Kuhn, P., Weis, W. I., Kobilka, B. K., and Stevens, R. C. (2007) High-resolution crystal structure of an engineered human β2-adrenergic G protein-coupled receptor. *Science 318*, 1258–1265.
37. McCusker, E. C., Bane, S. E., O'Malley, M. A., and Robinson, A. S. (2007) Heterologous GPCR expression: A bottleneck to obtaining crystal structures. *Biotechnol. Prog. 23*, 540–547.
38. Serrano-Vega, M. J., Magnani, F., Shibata, Y., and Tate, C. G. (2008) Conformational thermostabilization of the β1-adrenergic receptor in a detergent-resistant form. *Proc. Natl. Acad. Sci. U.S.A. 105*, 877–882.
39. Klammt, C., Schwarz, D., Eifler, N., Engel, A., Piehler, J., Haase, W., Hahn, S., Dotsch, V., and Bernhard, F. (2007) Cell-free production of G protein-coupled receptors for functional and structural studies. *J. Struct. Biol. 158*, 482–493.
40. Markkanen, P. M., and Petaja-Repo, U. E. (2008) N-Glycan-mediated Quality Control in the Endoplasmic Reticulum Is Required for the Expression of Correctly Folded δ-Opioid Receptors at the Cell Surface. *J. Biol. Chem. 283*, 29086–29098.
41. Kaushal, S., Ridge, K. D., and Khorana, H. G. (1994) Structure and function in rhodopsin: The role of asparagine-linked glycosylation. *Proc. Natl. Acad. Sci. U.S.A. 91*, 4024–4028.
42. Sung, C. H., Schneider, B. G., Agarwal, N., Papermaster, D. S., and Nathans, J. (1991) Functional heterogeneity of mutant rhodopsins responsible for autosomal dominant retinitis pigmentosa. *Proc. Natl. Acad. Sci. U.S.A. 88*, 8840–8844.
43. Morello, J. P., Salahpour, A., Laperriere, A., Bernier, V., Arthus, M. F., Lonergan, M., Petaja-Repo, U., Angers, S., Morin, D., Bichet, D. G., and Bouvier, M. (2000) Pharmacological chaperones rescue cell-surface expression and function of misfolded V2 vasopressin receptor mutants. *J. Clin. Invest. 105*, 887–895.
44. Morello, J. P., Petaja-Repo, U. E., Bichet, D. G., and Bouvier, M. (2000) Pharmacological chaperones: A new twist on receptor folding. *Trends Pharmacol. Sci. 21*, 466–469.
45. Esmann, M., Skou, J. C., and Christiansen, C. (1979) Solubilization and molecular weight determination of the (Na^++K^+)-ATPase from rectal glands of *Squalus acanthias*. *Biochim. Biophys. Acta 567*, 410–420.
46. Esmann, M. (1984) The distribution of C12E8-solubilized oligomers of the (Na^++K^+)-ATPase. *Biochim. Biophys. Acta 787*, 81–89.
47. Breyton, C., Tribet, C., Olive, J., Dubacq, J. P., and Popot, J. L. (1997) Dimer to monomer conversion of the cytochrome b6f complex. Causes and consequences. *J. Biol. Chem. 272*, 21892–21900.
48. Sarramegna, V., Muller, I., Milon, A., and Talmont, F. (2006) Recombinant G protein-coupled receptors from expression to renaturation: A challenge towards structure. *Cell. Mol. Life Sci. 63*, 1149–1164.

BI8018527